ISTANBUL UNIVERSITY –
JOURNAL OF ELECTRICAL & ELECTRONICS ENGINEERING

YEAR : 2008 (519-527)
VOLUME : 8
NUMBER : 1

DESIGN, OPTIMIZATION AND APPLICATION OF NOVEL PLANAR BENDING ESMAAs

YANG Kai, GU Cheng-lin

Huazhong University of Science and Technology, Wuhan 430074, Hubei Province, China
kkyhust@163.com

ABSTRACT

To overcome low response speed and low control precision in the existing traditional shape memory alloy actuators, the new type of structure named planar bending embedded shape memory alloy actuator was developed. Two SMA wires were embedded in parallel with the axis of the elastic rod. The actuating wire, which was superposed along rod's axis, was set to obtain "U" memory shape and the restoring wire, which was placed off-axially, got straight memory shape. The differential stain gauges were located at suitable position in corresponding to the actuator's bending direction in order to measure the signal of displacement. By making use of continuity, common origin and common limit conditions and adjusting martensite fraction coefficients appropriately, the analytical model was deduced to adequately account for the presence of major and minor hysteresis loops. The structural parameters of 60mm long actuator, such as rod's radius, wire's radius, wire's recoverable curvature and offset distance, were optimized by combining analytical model with experimental results. The experimental results prove the merits in optimal prototype.

I. INTRODUCTION

Actuators play a critical role in robotic system design and typically rely on electric, hydraulic or pneumatic technology. Unfortunately, there is a drastic reduction in the power that these forms of actuation can deliver as they are scaled down in size and weight. This restriction has opened up investigation of several novel actuator technologies such as those relying on piezoelectrics, polymer gels, magnetostrictive effects, electrostatics and SMA[2, 3].

Due to an SMA's capability of exerting high force and tolerating high strain, the use of SMAs in actuators is quite intriguing. The actuation of these devices is relatively simple since resistive heating from an electrical current can directly drive the SMA [4,5].

In 1984, Honma demonstrated that it is possible to control the amount of actuation by electric heating, thus opening their use in robotic application[6]. A skeleton muscle type robot was presented that consisted of a 5 degree of freedom (DOF) arm constructed of an aluminium-pipe skeleton operated with thin SMA fibres (0.2 mm) and bias springs. The end-effector of the robot was a gripper driven by a pair of antagonistic fibres. This is the earliest attempt of using SMA in an actuated robot arm. In the recent decade, several researchers have implemented shape memory technology for use in articulated hands. Hitachi produced a four-fingered robotic hand that incorporated 12 groups of 0.2mm fibres that closed the hand when activated. Dario proposed an articulated finger unit using antagonistic coils and a heat pump[7]. Gharaybeh and Burdea fitted several SMA springs to the Exos Dextrous Hand Master for use as a force feedback controller[8].

Considering the applications, there are several

Received Date: 11.09.2006
Accepted Date: 25.03.2008

disadvantages in the robot hands consisting of SMA actuators mentioned above. Firstly, the separation between actuating elements and executing elements is common in most configurations, which resulted in a complex structure and hampered their use in miniature systems. Secondly, their cartoon motions made grasping and fine manipulation very difficult. Thirdly, the response speed of SMA actuators is low due to the uncontrollable cooling process. To solve these problems, a new type of SMA actuator so called "Planar Bending ESMAA" is proposed as follows.

II. STRUCTURE

Fig.1 shows the prototype. Two SMA wires, with the same specification, are embedded in an elastic rod. The actuating wire w_1, with memorial 'U' shape, is located along the rod's axis. On the other hand, the restoring wire w_2, with memorial beeline shape, is located in parallel with the rod' axis with the offset distance d_1. If wire w_1 is heated by suitable current from pulse supply, the wire recovers to 'U' shape upon the temperature above A_s (the austenite phase transformation begin temperature). The rod will bend subsequently. When stop heating wire w_1 and heating wire w_2 by suitable current instead. The restoring force of wire causes the rod return to default straight immediately. So, the actuator possesses the ability to move in two directions and the movement is smooth, flexible and fast.

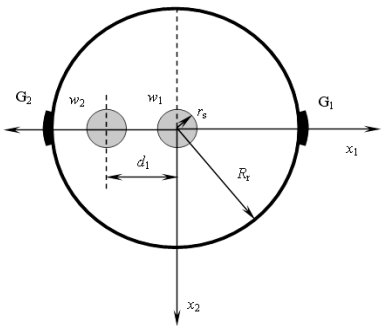

Fig.1 *Cross section of planar bending ESMAA*

To realize precise displacement control, the curvature sensor with two strain gauges is designed. As shown in Fig.1, the two strain gauges are arranged in complemental configuration. With the dimension 3mm in width and 5mm in length, the gauges stick to the center of rod's outside surface making use of 502 glue. When the actuator is actuated, the resistance varieties of two gauges have the same values. The final curvature's signal can be derived by a half measuring bridge in cooperating with the resistance varieties.

III. ANALYSIS MODEL

A. *Index of phase thansformation*

As we known, shape memory effect depends on the reversible transformation between two crystalline phases known as austenite (at high temperature) and martensite. The transformation is observed by noting the volume fraction of martensite R_m, which can vary between 0(all austenite) and 1(all martensite). Accordingly, R_m=1 indicates the alloy is in 100% martensite and R_m = 0 represents the alloy is in 100% austenite. The nonlinearity arises in the martensite fraction-temperature characteristic, $R_m(T)$, which is similar to the curvature-temperature characteristic, including the presence of major and minor hysteresis loops, which come from partial heating cycles. So, the determination of R_m is the key point of analysis model.

In our design, we adopt the exponential model, which relates the SMA martensite volume fraction to the temperature T and time t.

$$\begin{cases} R_{\mathrm{m}}^{\mathrm{H}}(T;t) = \dfrac{R_{\mathrm{ma}}^{\mathrm{H}}(t)}{[1+e^{k^{\mathrm{H}}(T-\beta^{\mathrm{H}})}]} + R_{\mathrm{mb}}^{\mathrm{H}}(t) \\ R_{\mathrm{m}}^{\mathrm{C}}(T;t) = \dfrac{R_{\mathrm{ma}}^{\mathrm{C}}(t)}{[1+e^{k^{\mathrm{C}}(T-\beta^{\mathrm{C}})}]} + R_{\mathrm{mb}}^{\mathrm{C}}(t) \end{cases} \quad (1)$$

For convenience, let the superscript C denote "cooling" and the superscript H denote "heating". Since it is assumed that natural convection is used to cool the wire, the wire temperature cannot fall below the ambient temperature. Also, define two "temperature constants" k^C and k^H.

In any physical SMA material both k^C and k^H are positive. The piecewise-constant functions of time, $R_{ma}(t)$ and $R_{mb}(t)$ are available for different hysteresis loops. As long as the wire is just being heated or just being cooled, the functions $R_{ma}^{C}(t)$ 、 $R_{mb}^{C}(t)$ 、 $R_{ma}^{H}(t)$ and $R_{mb}^{H}(t)$ remain constant. It is only when the wire goes from heating to cooling, or vice-versa, that these functions change.

B. shape change model for rod

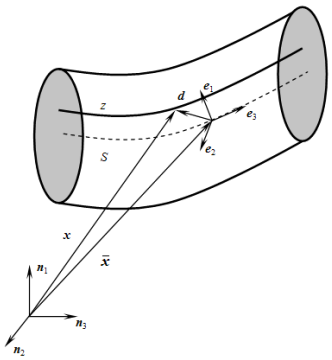

Fig.2 *Force analysis of wire and rod*

As shown in fig.2, the vector form of the equations of equilibrium of a flexible rod acted upon by a distributed force, f, acting at a distance d from the centoid, is(Love 1994, Tadjbakhsh and Lagoudas 1993)[9,10]

$$\frac{\mathrm{d}\boldsymbol{F}}{\mathrm{d}S}+\boldsymbol{f}=0 \tag{2}$$

$$\frac{\mathrm{d}\boldsymbol{M}}{\mathrm{d}S}+\frac{\mathrm{d}\bar{\boldsymbol{x}}}{\mathrm{d}S}\times\boldsymbol{F}+\boldsymbol{m}=0 \tag{3}$$

where F is the rod resultant force vector and M is the rod resultant moment vector. The distributed force, f, applied on the rod from the wire is connected through Newton's third law to the distributed force, f', applied from the rod to the actuator by

$$f=-\frac{dz}{ds}f' \tag{4}$$

The vector form of the equations of equilibrium for the wire is

$$\frac{\mathrm{d}\boldsymbol{F}^{\mathrm{a}}}{\mathrm{d}z}+\boldsymbol{f}'=0 \tag{5}$$

From the operation principle of the actuator, it is obvious that only one wire, w_1 or w_2, is actuated at one time. Consequently, the movement of the actuator upon w_2 being heated is examined in the detail. Since the process for the rod from "U" shape to straight has the entirely reverse behavior with the process from straight to "U" shape, the characteristics for rod's bending upon w_2 being heated are investigated as follows.

Equation (5) has in general the following resolution in the osculating plane

$$\frac{\mathrm{d}F^{\mathrm{a}}}{\mathrm{d}z}\boldsymbol{n}+F^{\mathrm{a}}\frac{\mathrm{d}\boldsymbol{n}}{\mathrm{d}z}+f_{\mathrm{t}}\boldsymbol{t}+f_{\mathrm{n}}\boldsymbol{n}=0 \tag{6}$$

where t is the tangent unit vector and n is the principal normal vector. If the trihedral basis is used to resolve the vector form of the equations of equilibrium into components, the following set of two equations obtains by equation (6)

$$\frac{\mathrm{d}F^{\mathrm{a}}}{\mathrm{d}z}+f_{\mathrm{n}}=0 \tag{7}$$

$$-k_2F^{\mathrm{a}}+f_{\mathrm{t}}=0 \tag{8}$$

The distributed forces acting on the rod are given by $f_1=-f_{\mathrm{n}}$, $f_3=-f_{\mathrm{t}}$ and $m_2=-d_1f_3$. Appling equations (7)-(8) to equations (2)-(3), then

$$\frac{\mathrm{d}F_1}{\mathrm{d}S}+k_2F_3+\frac{\mathrm{d}F^{\mathrm{a}}}{\mathrm{d}z}=0 \tag{9}$$

$$\frac{\mathrm{d}F_3}{\mathrm{d}S}-k_2F_1-k_2F^{\mathrm{a}}=0 \tag{10}$$

$$\frac{\mathrm{d}M_2}{\mathrm{d}S}+(1+e)F_1+d_1k_2F^{\mathrm{a}}=0 \tag{11}$$

If the elongation of rod is negligible, and the direction of wire's actuating force is along the principal normal vector that F_3 is approximatively taken as zero, the equations (9)-(11) reduce to

$$F_1+F^{\mathrm{a}}=0 \tag{12}$$

$$\frac{\mathrm{d}M_2}{\mathrm{d}S} - (1 - d_1 k_2) F^{\mathrm{a}} = 0 \tag{13}$$

Combining with the experimental results, the distributed forces from "U" shape actuating wire can be regarded as the force of uniformly distributed load. So, according to beam theory, the wire's recoverable curvature and actuating force have the expressions

$$k' = \frac{qL^2}{8E^{\mathrm{a}} I^{\mathrm{a}}} \tag{14}$$

$$F^{\mathrm{a}} = qx \tag{15}$$

where E^{a} , I^{a} are Young's moduli and moment of inertia of the cross-section of the wire. q, L are load density and wire length respectively. The distance from calculation point to reference point is denoted by x.

The moment M_2 obtains making use of equations (13)-(15)

$$M_2 = (1 - d_1 k_2) k' E^{\mathrm{a}} I^{\mathrm{a}} \tag{16}$$

Since the following constitutive assumption is made using beam theory

$$M_2 = EIk_2 \tag{17}$$

where E, I are Young's moduli and moment of the cross-section of the rod respectively. Then, the recovering curvature of wire is derived using equations (16)-(17)

$$k_2 = \frac{k' E^{\mathrm{a}} I^{\mathrm{a}}}{EI + d_1 k' E^{\mathrm{a}} I^{\mathrm{a}}} \tag{18}$$

Defining a constant

$$\alpha = \frac{EI}{E^{\mathrm{a}} I^{\mathrm{a}}}$$

Then the equation (18) can be rewritten as

$$k_2 = \frac{k'}{\alpha + d_1 k'} \tag{19}$$

w_2 serves as restoring wire with remembered straight shape, and the bending curvature is calculated as

$$k_2' = R_{\mathrm{m}} k'_{\max 2} \tag{20}$$

where $k'_{\max 2}$ is the maximum, which keeps the following relation with the actuator's maximum curvature $k_{\max}$

$$k_{\max} = \frac{k'_{\max 2}}{\alpha + d_1 k'_{\max 2}} \tag{21}$$

The actuators' curvature upon heating wire w_2 obtains by equations (19)-(21)

$$k_2 = \frac{R_{\mathrm{m}} k'_{\max 2}}{\alpha + d_1 R_{\mathrm{m}} k'_{\max 2}} \tag{22}$$

When wire w_1 is heated: d_1=0 and m_2=0. The equations (9)-(11) can be rewritten as

$$F_1 + F^{\mathrm{a}} = 0 \tag{23}$$

$$\frac{\mathrm{d}M_2}{\mathrm{d}S} - F^{\mathrm{a}} = 0 \tag{24}$$

Similarly, the curvature of actuator is

$$k_2 = \frac{k'}{\alpha} \tag{25}$$

The relationship between actuator's curvature and martensite fraction R_{m} can be calculated by the following formula

$$k_2 = \begin{cases} \dfrac{(1 - R_{\mathrm{m}}) k'_{\max}}{\alpha} & w_1 \text{ is heated} \\ \dfrac{R_{\mathrm{m}} k'_{\max 2}}{\alpha + d_1 R_{\mathrm{m}} k'_{\max 2}} & w_2 \text{ is heated} \end{cases} \tag{26}$$

IV OPTIMAI DESIGN OF STRUCTURE

It is explicit that the maximum curvature of actuator greatly depends on the rod's radius, wire's radius, wire's recoverable curvature and restoring wire's offset distance. Neglecting the temperature disturbance and bending resistance of restoring wire when the actuating wire is heated, the simulated relations between actuator's maximum curvature and rod's radius, wire's radius, wire's recoverable curvature and offset distance obtain from the model mentioned above. All results will provide powerful instructions for the design of prototypes.

Fig.3 is the relation between actuator's maximum curvature $k_{\max}$ and the rod's radius R_{r}. It is obvious that maximum curvature, $k_{\max}$, is decreasing with increasing of the rod's radius, Rr.

Since the load ability depress greatly along with decreasing of *R*r, there should be an optimal value. Considering that the actuator is used for anthropopathic robot hand, R_r is choosed as 5mm, which is comparative with the hand of human being.

The rod's radius and wire's recoverable curvature are set as 5m and $57m^{-1}$ respectively. The relation between k_{max} and the wire's radius r_s as shown in fig.4. In the figure, k_{max} is increasing with the decreasing of r_s exponentially. When r_s is less than 0.25mm, the increase of r_s has great influence on k_{max}. On the contrast, after r_s is above 0.25mm, the effect weakens rapidly. Although k_{max} can be increased obviously through increasing r_s, the response speed slows down and actuator's remnants curvature after the temperature of actuator falls below room temperature is biggish. Therefore, to find an optimal value for wire's radius, an index is defined as

$\alpha=k_{max}/k_{left}$ where k_{left} is remnants curvature. Fig.5 is the simulated result of the index versus wire's radius r_s. It is interesting to see that the optimal radius is around 0.3mm. So, the 0.25mm in radius wire is choosed as the actuation wire from the materials we can get.If r_s=0.25 and R_r=5mm, from the model, the relation of k_{max} versus the wire's recoverable curvature k_r is nearly linear. So, it is explicit that increasing k_r is the most effective way to increase k_{max}. In order to meet the requirement of displacement range and boundary condition of wire's prestrain, the wire's recoverable curvature, k_r, is set as $57m^{-1}$ at last.

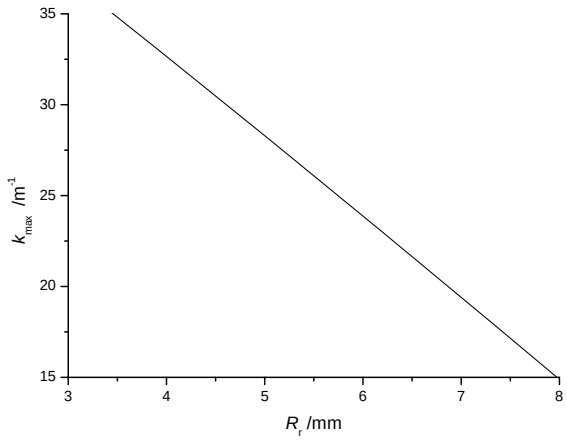

Fig.3 *Relation between maximum curvature and rod's radius*

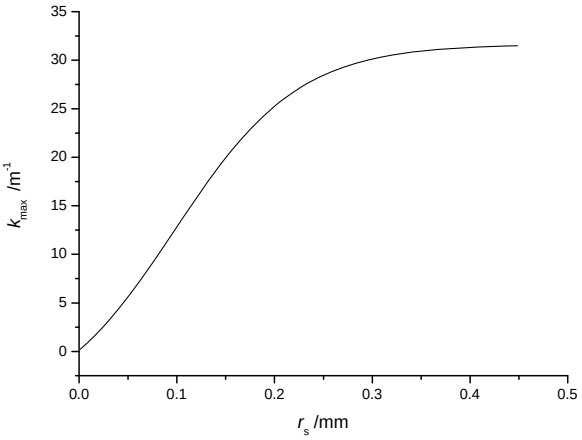

Fig.4 *Relation between maximum curvature and wire's radius*

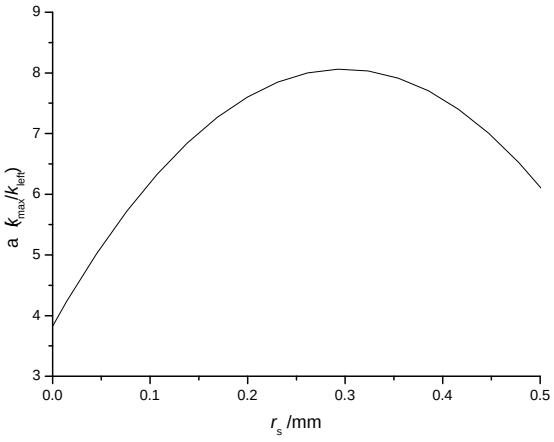

Fig.5 *Index a as a function of wire's radius*

In the planar bending ESMAA, there are two embedded wires, i.e., w_1 and w_2. Since wire w_2 serves as restoring wire with memorial beenline shape, it is also important to determine the off-axial distance, d, of the wire away from rod's centerline. Choose r_s=0.25mm, R_r=5mm, k_r=57m^{-1} and straighten w_2 carefully before embedding it into the rod, the relaition of k_{max} versus d is shown in fig.6. From the figure, it is explicit that when the off-axial distance, d, is small, wire w_2 return the rod to straight line quickly. On the other hand, too small distance will result in heat disturbance between w_1 and w_2. Considering restrictions mentioned above synthetically, d=3mm is appropriate. Finally, the material and geometrical parameters of designed prototype are summarized below and in table.1.

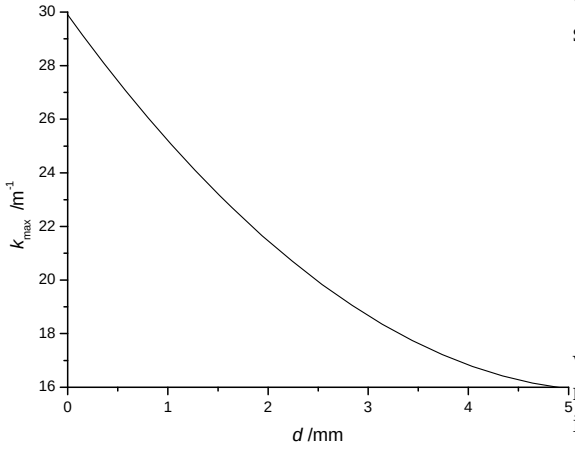

Fig.6 *Relation between maximum curvature and off-axial distance*

TABLE 1: *Geometrical and material parameters of prototype*

Names	Values
Rod's elastic modulus, E (MPa)	0.78
Rod's radius, R_r (mm)	5
Wire's austenitic elastic modulus (GPa)	83.3(E_A)
Wire's martensite elastic modulus(GPa)	60.5(E_M)
Off-axial distance (mm)	3
Wire's radius, r_s (mm)	0.25
Wire's recoverable curvature, k_r (m^{-1})	57
Length (mm)	60

V. EXPERIMENTAL RESEARCH

A. Response Speed

The bending of ESMAAs attributes to the phase transformation of SMA wires, w_1 and w_2, which is caused by heating and cooling cycle. The phase transformation of SMA wires from martensite to austenite is induced by electrical heating. The cooling experiments were carried out on the ESMAA prototype with 0.25mm in wire's radius and 5mm in rod's radius. The actuator experienced different cooling conditions, i.e. air cooling, wind cooling and water cooling after its curvature reached the maximum 28.5m^{-1}. Besides experiments mentioned above, the time, within that the actuator restored to line by heating wire w_2 from maximum bending state, was measured. All tested restoring time were summarized in table.2.

TABLE 2: *Restoring time for different conditions*

Conditions	Restoring time (s)
Air cooling	3
Wind cooling	2.5
Water cooling	2
Heating wire w_2	0.8

From the above table, the former three values were similar since wire w_1 was embedded in the rod and the cooling conditions could not influence it directly. So, it is not a perfect

measure to increase the response speed of ESMAA through external cooling condition. Fortunately, the restoring time fell down drastically when wire w_2 was heated. It is no doubt that the designed ESMAA has enhanced performance in rapid response speed.

B. Step Response

Most actuator applications require displacing an object against an opposing force, such as moving an actuator limb coupled to a load. So accurate and rapid position control has to be implemented. The actuator's curvature and current duty ratio respectively when a "proportional-diode" controller is added to the system are simulated in fig.7 and fig.8. Proportional gain, K_p=0.05, and sampling period, T_s, of 15.4 milliseconds, are used. The model exactly provides reasonable agreement with the corresponding experimental results in fig.9 and fig.10. Note in particular that the model predicts a similar steady-state error. Reducing the heat transfer coefficient, an important parameter in the temperature-current relation of actuating wire, may improve the correlation between the simulated and experimental results, since such a reduction in the parameter would mean that heat, in the model, would be lost to the air less readily. Hence, small duty ration of current would be required to maintain the same wire temperature.

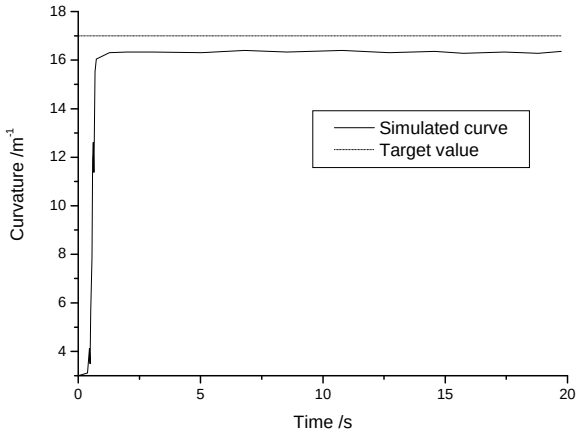

Fig.7 *Simulated step response using P^+ control*

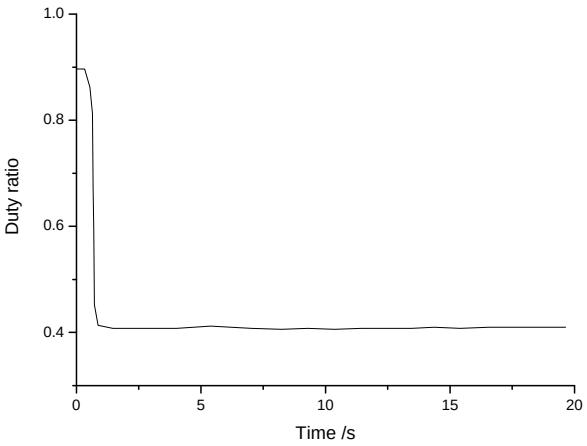

Fig.8 *Simulated duty ratio of current using P^+ control*

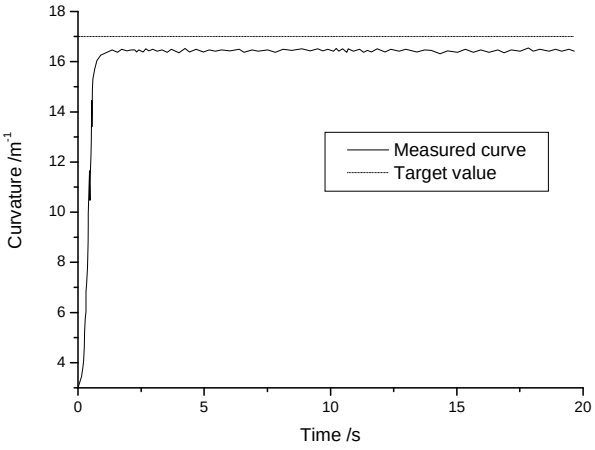

Fig.9 *Experimental step response using P^+ control*

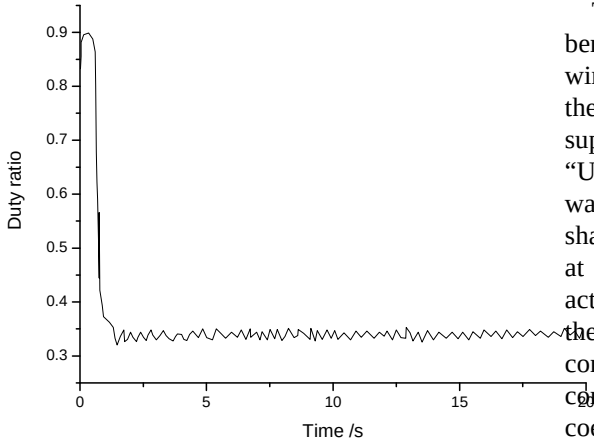

Fig.10 *Experimental duty ratio of current using P^+ control*

To verity the basic performance of this ESMAA, the anthropopathic robot hand consisting of six ESMAAs was built. The driving experiment was conducted on a sphere weight of 3N with a 15mm radius of the sphere, as shown in fig.11. The novel hand's finger tip was shown to make a pliable motion with about 115 degree/second up to a designed maximum angle (75 degrees) at the responding speed high enough for the purpose. By controlling the bending of each finger, the hand could accomplish fine manipulation like that of a human being.

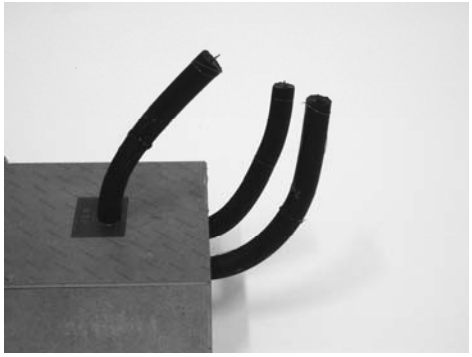

Fig.11 *Anthropopathic hand consisting of ESMAAs*

VI. CONCLUSION

The new type of structure named planar bending ESMAA was developed. Two SMA wires were embedded in parallel with the axis of the elastic rod. The actuating wire, which was superposed along rod's axis, was set to obtain "U" memory shape and the restoring wire, which was placed off-axially, got straight memory shape. The differential stain gauges were located at suitable position in corresponding to the actuator's bending direction in order to measure the signal of displacement. By making use of continuity, common origin and common limit conditions and adjusting martensite fraction coefficients appropriately, the analytical model was deduced to adequately account for the presence of major and minor hysteresis loops. The structural parameters of the actuator, such as rod's radius, wire's radius, wire's recoverable curvature and offset distance, were optimized by combining analytical model with experimental results. An actuator prototype has been constructed with the following properties:

- Light weight - 2.5 grams
- Compact - 10 mm cylinder×60 mm long
- Big curvature -18m^{-1}
- Direct drive actuator
- Smooth movements

The response speed and step experiments were carried out to prove the merits of model. Using the actuators, a three-fingered anthropopathic robot hand was designed to accomplish anthropomorphic grasping and fine manipulations. The maximum bending angle of one finger tip was about 75^o when the duty ratio was 70 percent. The prototype can grasp a sphere 15mm in radius. The motions are flexible and lifelike. A clear picture of the grasping experiment shows that the fingertip could reach the set point fast and precisely.

VII REFERENCES

[1] Elahinia M H, Ashrafiuon H, Ahmadian M *et al*. A temperature-based controller for a shape memory alloy actuator[J]. Journal of Vibration and Acoustics, 2005, 127(3):285-291

[2] Liu Jianfang, Yang Zhigang, Cheng Guangming *et al*. A study of precison PZT line setp motor[J]. Proceedings of the CSEE,

2004, 24(4):102-106

[3] Han L H, Lu T J, Evans A G. Optimal design of a novel high authority SMA actuator[J]. Mechanics of Advanced Materials and Structures, 2005, 12(3): 217-227

[4] Singh K, Sirohi J, Chopra I. An improved shape memory alloy actuator for rotor blade tracking[J]. Journal of Intelligent Material Systems and Structures, 2003, 14(12):767-786

[5] Kumagai A, Hozian P, Kirkland M. Neuro-Fuzzy Based Feedback Controller for Shape Memory Alloy Actuators[C]. Proc SPIE Int Soc Opt Eng, Newport Beach CA USA, Mar.6-9 2000(5): 291-299

[6] Hirose S, Ikuta K, Umetani Y. New design method of servo-actuators based on the shape memory alloy effect[M]. Cambridge MA USA, MIT Press, 1985

[7] Menciassi A, Pernorio G., Dario P. A SMA actuated artificial earthworm . IEEE International Conference on Robotics and Automation, 2004(4):3282-3287

[8] M. A Gharaybeh and G.C. Burdea. Investigation of a shape memory alloy actuator for dextrous force-feedback masters. Advanced robotics, 1995 (3):317-329

[9] Dimitris C Lagoudas and Tradj G Tadjbakhsh. Active flexible rods with embedded SMA fibers. Smart Mater.Struct, 1992(1):162-167

[10]Brett De Blonk, Andrew J.Kurdila, Dmitris C lagoudas and Glenn Webb. Identification of the transient response of SMA embedded flexible rods: SPIE, 1995(2443):335-34